2017 14th Workshop on Positioning, Navigation and Communications (WPNC)

Coarse Estimation of the Incident Angle for VLP with an Aperture-Based Receiver

Sander Bastiaens, Heidi Steendam
Ghent University, Ghent, Belgium. (E-mail: firstname.lastname@ugent.be).

***Abstract*—Recently, an estimation algorithm for the angle-of-arrival (AoA) for visible light positioning (VLP) was investigated [1]. In this paper, the authors considered an aperture-based receiver, and estimated for each light beacon the incident angle and polar angle between the beacon and the receiver using an iterative maximum likelihood (ML) based algorithm. For the iterative ML algorithm to converge, an accurate initial estimate was required. To obtain this initial estimate, a coarse ad hoc estimation algorithm for the incident angle was proposed. However, the proposed estimator for the incident angle was not able to deliver sufficiently accurate estimates for a wide range of incident angles, resulting in slow convergence of the iterative algorithm and large positioning errors. In this paper, we propose three novel estimators for the incident angle that are not only more accurate than the coarse estimator proposed in [1], but also have a wider estimation range.**

***Index Terms*—VLP, positioning, angle-of-arrival, incident angle, coarse estimator**

I. Introduction

Indoor positioning has attracted a lot of attention during the last decade, both in research and commercial applications. As humans spend a large part of their lives indoors, many applications are being developed that employ the indoor position of a user or object. Several indoor positioning techniques are being considered, but hardly any of those approaches combines a low cost and a low power consumption with a high accuracy. Visible light positioning [2]-[17] has the potential to fulfil these requirements. Moreover, it holds several advantages over other positioning technologies, e.g. all indoor environmental safety and applicability, privacy and the possibility for widespread deployment, due to solid state lighting currently revolutionizing the illumination infrastructure.

Several techniques for VLP consider a two-step approach. Firstly, position-related information such as the distance between the receiver and a beacon, or the direction of the incident light, is extracted from the received signal. In a second step, the position of the receiver is determined using geometrical techniques such as trilateration or triangulation. The position-related information can be obtained by measuring the time-of-arrival (ToA), by evaluating the received signal strength (RSS) or by determining the angle-of-arrival (AoA). As ToA requires very accurate synchronization between the transmitter and the receiver and as RSS based techniques need the knowledge of the transmitted optical signal strength, both of which is hard to obtain, the most promising approach for VLP considers the AoA.

To measure the AoA, either the transmitter or the receiver must be directional. In order to reduce the installation cost, the existing illumination infrastructure will be adapted to also support positioning. As most light fixtures have a wide field-of-view to allow uniform illumination over a room with a limited number of fixtures, we have to resort to directional receivers that can distinguish the direction from the incident light. In this paper, we focus on the directional aperture-based receiver introduced in [18] for MIMO visible light communication (VLC).

The receiver from [18] was considered for AoA-based VLP in [19], where the Cramer-Rao bound (CRB) on the AoA was determined. In [1], an algorithm was proposed that estimates the AoA and that obtains the user's position in three dimensions (3D). The algorithm iteratively searches for the optimal AoA starting from an initial AoA estimate. In order for the iterative algorithm to converge, accurate initial AOA estimates are required. In [1], a coarse estimator for the AoA was introduced, but the proposed ad hoc algorithm for the incident angle is only able to deliver an accurate estimate within a limited range of the incident angle. This resulted in slow convergence of the iterative algorithm and large positioning errors. In this paper, several novel coarse estimators for the incident angle will be introduced, in order to both improve the accuracy of the incident angle estimate and to extend the range over which reliable estimates can be obtained.

II. System Description

The considered VLP system incorporates three elements: the transmitter, the optical channel and the receiver. In Section II-A, the signals broadcast by the transmitter will be described, while in Section II-B, the receiver and the optical channel will be considered.

A. Transmitter

The positioning infrastructure consists of K white LEDs that are attached to the ceiling at well-known positions $(x_{S,i}, y_{S,i}, z_{S,i})$. The LEDs are assumed to point downwards and are modelled as Lambertian radiators with order m_i, $i = 1, \ldots, K$. In the positioning system, the receiver must be able to separate the contributions from the different LEDs. Hereto, each LED broadcasts a different dc-biased sinusoid waveform $s_i(t)$, $i = 1, \ldots, K$:

$$s_i(t) = A_i \left(1 + \cos(2\pi f_{c,i} t + \theta_i)\right), \tag{1}$$

where the signals from the different LEDs are assumed to be unsynchronized, i.e. the phase differences θ_i are random variables that are uniformly distributed in the interval $[0, 2\pi]$. This assumption will simplify the installation of the LED beacons. The receiver will observe the signals during a time interval with duration T. In order to avoid interference between the signals at the receiver, the frequencies $f_{c,i}$ are selected to be orthogonal over this time interval. The frequencies must be sufficiently large to prevent flickering detectable by the

978-1-5386-3089-1/17/$31.00

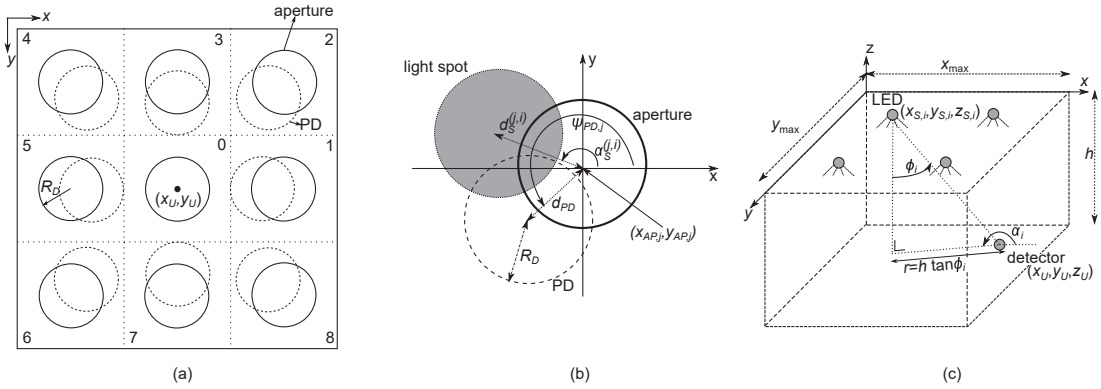

Fig. 1. a) Top view of the receiver with $M = 9$ REs, b) one RE, and c) definition of the incident and polar angle (ϕ_i, α_i).

human eye: we consider frequencies $f_{c,i}$ in the interval 2kHz-20kHz. Further, to allow real-time operation, we assume that the duration T of the time interval is of the order of 1-10ms.

B. Receiver

The directional receiver consists of $M = 9$ receiving elements (REs), where each RE contains a circular photodiode (PD) and a circular aperture. The radii of the photodiodes and apertures are all equal to R_D. The apertures are arranged in a square grid, as shown in Fig. 1a. The PDs are allocated in a plane at a distance h_A below the plane of the apertures. For all REs, except for the centre RE where the PD is placed just below the aperture, the PD is displaced compared to its corresponding aperture in order to change the field-of-view of the RE. The radius R_D is large compared to the wavelength of the light, and we assume that the light that reaches a PD has to come through its aperture. Hence, the light coming through an aperture will introduce a circular light spot on the plane of the PDs, as shown in Fig. 1b.

The receiver origin (x_U, y_U, z_U), which is the reference point to be determined in the positioning process, coincides with the centre of the central aperture. Further, AoAs are defined between the receiver and LED i as

$$\begin{aligned} x_{S,i} - x_U &= (z_{S,i} - z_U)\tan\phi_i \cos\alpha_i \\ y_{S,i} - y_U &= (z_{S,i} - z_U)\tan\phi_i \sin\alpha_i, \end{aligned} \tag{2}$$

where ϕ_i is the incident angle and α_i is the polar angle (Fig. 1c). To estimate the AoAs for the different LEDs, we need to evaluate the received signal strength in each PD. When multiple LEDs are simultaneously broadcasting signals, first the contributions from the different signals must be separated. If we simply correlate the outputs of the PDs with the signals $\eta_i(t) = \cos(2\pi f_{c,i} t)$:

$$\int_0^T s_i(t)\eta_{i'}(t)dt = \frac{A_i T}{2}\cos\theta_i \delta_{i,i'}, \tag{3}$$

the output of the correlation is a function of the unknown phase θ_i. To remove the dependency on the phase θ_i, we use a sliding window correlation, and take the maximum of this correlation over one period of $\eta_i(t)$. In that case, the output s_i of the PD corresponding to the contribution of LED i becomes independent of θ_i:

$$s_i = \frac{A_i T}{2}. \tag{4}$$

From (3), it can be observed that, due to the orthogonality of the frequencies $f_{c,i}$, the sliding window correlation with the function $\eta_i(t)$ will only contain the contribution of LED i. Gathering the results of the correlation of the received signal with the K functions $\eta_i(t)$ at the M PDs, yields the vector of observations $\mathbf{r} = (\mathbf{r}_1^T \ldots \mathbf{r}_M^T)^T$ where

$$\mathbf{r}_j = (r_{j,1} \ldots r_{j,K})^T, j = 0, \ldots, M-1 \tag{5}$$

and

$$r_{j,i} = R_p h_c^{(j,i)} s_i + n_{j,i}. \tag{6}$$

In this expression, R_p is the responsitivity of the PD, $h_c^{(j,i)}$ is the channel gain from LED i to PD j and $n_{j,i}$ is the noise contribution. We assume that the noise is dominated by shot noise and that this shot noise can be modelled as zero-mean Gaussian noise with covariance $E[n_{j,i}n_{j',i'}] = \frac{N_0 T}{2}\delta_{i,i'}\delta_{j,j'}$ and spectral density $N_0 = 2qR_p p_n A_D \Delta\lambda$ [20], where q is the charge of an electron, p_n the background spectral irradiance, A_D the area of the PD and $\Delta\lambda$ the bandwidth of the optical filter placed in front of the PD.

The channel gain $h_c^{(j,i)}$ depends on the positions of the apertures and the PDs. The apertures are placed on a square grid at positions $(x_{AP,j}, y_{AP,j}, z_{AP,j}) = (x_U + \delta x_j, y_U + \delta y_j, z_U), j = 0, \ldots, 8$, where $\delta x_j = \epsilon\,(0\ \ 1\ \ 1\ \ 0\ \ -1\ \ -1\ \ -1\ \ 0\ \ 1)$ and $\delta y_j = \epsilon\,(0\ \ 0\ \ 1\ \ 1\ \ 1\ \ 0\ \ -1\ \ -1\ \ -1)$. All PDs, except the centre PD, are slightly displaced with respect to their apertures. To obtain a receiver with a large and symmetrical field-of-view, we select the positions of the PDs $(x_{AP,j} + x_{PD,j}, y_{AP,j} + y_{PD,j}, z_U - h_A)$ with $x_{PD,0} = y_{PD,0} = 0$ and $(x_{PD,j}, y_{PD,j}) = (d_{PD}\cos\psi_{PD,j}, d_{PD}\sin\psi_{PD,j})$ where $\psi_{PD,j} = \pi + (j-1)\frac{\pi}{8}$, $j = 1, \ldots 8$. In this paper, we assume $\epsilon = 5R_D$. Simulations have shown that the placement of the apertures has a negligible effect on the performance, as long as the assumption that the only light that reaches a PD is the light coming through its PD, is fulfilled.

We assume the receiver is parallel to the ceiling. Similarly as the AoAs ϕ_i and α_i, we can define the incident angle $\phi_{j,i}$ and polar angle $\alpha_{j,i}$ between PD j and LED i:

$$\begin{aligned} x_{S,i} - x_{AP,j} &= (z_{S,i} - z_{AP,j})\tan\phi_{j,i}\cos\alpha_{j,i} \\ y_{S,i} - y_{AP,j} &= (z_{S,i} - z_{AP,j})\tan\phi_{j,i}\sin\alpha_{j,i}. \end{aligned} \tag{7}$$

Using (7), the channel gain can be written as [20]

$$h_c^{(j,i)} = \frac{m_i+1}{2\pi(z_{S,i}-z_U)^2} A_0^{(j,i)} \cos^{m_i+3}\phi_{j,i}, \tag{8}$$

where $A_0^{(j,i)}$ is the overlap area between PD j and the light spot coming from LED i:

$$A_0^{(j,i)} = \begin{cases} 2R_D^2 \arccos\left(\frac{d_{j,i}}{2R_D}\right) & 0 \le d_{j,i} \le 2R_D \\ -\frac{d_{j,i}}{2}\sqrt{4R_D^2 - d_{j,i}^2} & \\ 0 & d_{j,i} > 2R_D. \end{cases} \tag{9}$$

where the distance between the PD's and the light spot's centre $d_{j,i}$ satisfies

$$d_{j,i} = \sqrt{\Delta x^2 + \Delta y^2}, \tag{10}$$

with

$$\begin{aligned} \Delta x &= x_{PD,j} - d_S^{(j,i)} \cos\alpha_S^{(j,i)} \\ \Delta y &= y_{PD,j} - d_S^{(j,i)} \sin\alpha_S^{(j,i)}, \end{aligned} \tag{11}$$

and $d_S^{(j,i)} = h_A \tan\phi_{j,i}$ and $\alpha_S^{(j,i)} = \pi + \alpha_{j,i}$.

III. Coarse Estimation of the Incident Angle ϕ

To determine the position of the receiver, we can estimate the AoA for each LED and use triangulation to determine the position. In [1], an algorithm is proposed based on the maximum likelihood principle, which iteratively estimates the AoAs, by comparing the relative differences between the RSS values in the different PDs. Hence, the receiver does not require the knowledge of the transmitted optical power. In order to converge, this algorithm needs an accurate initial estimate for α_i and ϕ_i. However, the coarse estimator from [1] showed some deficiencies. Firstly, the coarse estimator had difficulties to distinguish the case where the LED was just above the receiver. To cope with this problem, in this paper, we introduced a receiver with a centre RE. By comparing the RSS value of the centre PD with those of the other PDs, we can easily decide whether the receiver is just below a LED or the RSS values are dominated by noise. Secondly, the coarse estimator for the incident angle ϕ_i from [1] can only estimate ϕ_i for a limited range of angles, and exhibits a significant mean squared error. This will affect the positioning accuracy and the convergence rate of the algorithm. In this section, several alternative estimators are proposed, which will provide more accurate coarse estimates of ϕ_i and will extend the range over which a reliable estimate for ϕ_i can be obtained.

In order to derive novel coarse estimators for the incident angle ϕ_i, we take a closer look at the RSS values in the different PDs. If the signal coming from LED i is not dominated by noise and, if we do not take into account the centre RE with index $j = 0$ and only look at the outer REs with $j \in [1, 8]$, the three largest of the outer RSS values will occur in three adjacent REs, with the maximum of these RSS values occurring in the middle of the three. If this is not the case, we need to look at the centre PD: if the RSS value in this PD is larger than for the outer PDs, we decide that the receiver is just below the LED, while if it is lower, we decide the signal is noise dominated. In this latter case, the resulting RSS values are not reliable and cannot be used for positioning. This will happen if the incident angle ϕ_i is larger than $\phi_{out} \approx \text{atan}\frac{2R_D+d_{PD}}{h_A}$, as in that case none of the REs will receive light from the LED, i.e. the LED is out of the field-of-view of the receiver. The angle ϕ_{out} defines a cone with as apex the LED and apex angle $2\phi_{out}$, within which the receiver can see the LED. The coarse estimators can therefore only return an estimate for ϕ_i if $\phi_i \le \phi_{out}$.

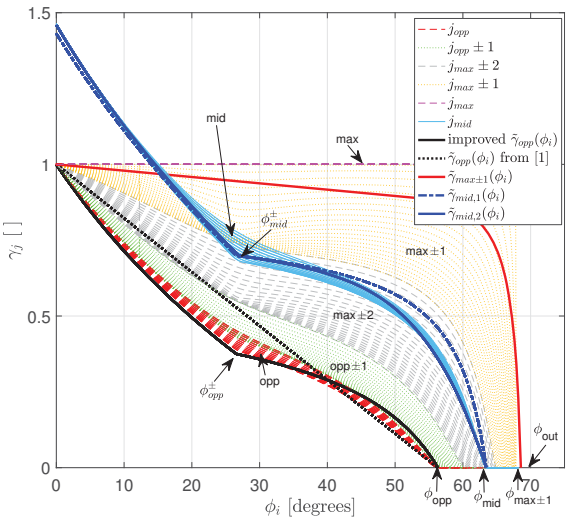

Fig. 2. The ratio γ_j as function of the incident angle ϕ_i for $\epsilon = 5R_D$, $d_{PD} = 0.5R_D$ and $h_A = R_D = 1$ mm. $\phi_{\text{opp}} = 56.3$ degrees and $\phi_{out} = 68.2$ degrees.

In [1], the estimation of ϕ_i was based on the evaluation of the ratio of RSS values $\gamma_j = \frac{r_{j,i}}{r_{\max,i}}$, where $r_{\max,i}$ is the maximum of the RSS values, i.e. $r_{\max,i} = \max_j r_{j,i}$. In this paper, where we have a centre PD, we define a similar ratio:

$$\gamma_j = \frac{r_{j,i}}{r_{\max,8}}, \quad \text{with } r_{\max,8} = \max_{j\in[1,8]} r_{j,i}, \tag{12}$$

where the RSS values $r_{j,i}$ are compared with the largest RSS in the outer PDs, $r_{\max,8}$ with index $j = j_{\max}$. In Fig. 2, this ratio γ_j is shown as function of ϕ_i, assuming no shot noise is present. Different lines with the same colour correspond to different values of α_i. As can be observed, the curves for j_{opp} show the smallest spread for different values of α_i. Because of this, in [1], $\gamma_{\text{opp}} \stackrel{\Delta}{=} \gamma_{j_{\text{opp}}}$ was evaluated to obtain a coarse estimate for ϕ_i, where j_{opp} is the index of the RE opposite to the RE $j_{\max}$ with maximum RSS value. In [1], γ_{opp} was modelled as a linear function of ϕ_i, i.e.

$$\gamma_{\text{opp},[1]} \approx 1 - \frac{\phi_i}{\phi_{\text{opp}}}, \tag{13}$$

where $\phi_{\text{opp}} \approx \text{atan}\frac{2R_D-d_{PD}}{h_A}$ is the incident angle above which RE j_{opp} no longer receives light from the LED. This approximation is illustrated in Fig. 2. It can be observed that a large gap exists between (13) and the true γ_{opp}, implying this coarse estimator will have a large mean squared error. The first coarse estimator for ϕ_i, proposed in this paper, solves this issue by considering a better approximation for γ_{opp}, with which a more accurate estimate for ϕ_i can be obtained. To this end, we first notice that the distances on the receiver are

in general much smaller that the distance between the LED and the receiver, i.e. $\delta x_j, \delta y_j \ll z_{S,i} - z_U$. In that case, the incident angles $\phi_{j,i}$ and polar angles $\alpha_{j,i}$ are approximately equal to ϕ_i and α_i, respectively. Because of this, the ratio γ_j can be approximated as

$$\gamma_j \approx \frac{A_0^{(j,i)}}{A_0^{(j_{\max},i)}}. \tag{14}$$

The area of overlap $A_0^{(j,i)}$ is a non-linear function of ϕ_i and α_i. Note that this ratio is essentially independent of the Lambertian order m_i of the LED. For $0 \leq d_{j,i} \leq 2R_D$, $A_0^{(j,i)}$ can be approximated as

$$A_0^{(j,i)} \approx \pi R_D^2 \left(1 - \frac{d_{j,i}}{2R_D}\right)\left(1 - \frac{d_{j,i}}{4R_D}\right) \tag{15}$$

Taking into account that $d_{j_{\text{opp}},i} \approx d_{PD} + h_A \tan\phi_i$ and $d_{j_{\max},i} \approx |d_{PD} - h_A \tan\phi_i|$, we obtain the estimate (16), where $\zeta = d_{PD}/R_D$, $\lambda = \frac{1+\gamma_{\text{opp}}}{1-\gamma_{\text{opp}}}$ and where $\gamma_{\text{opp}}^{\pm} = (1-\zeta)(1-\zeta/2)$ corresponds to the $\phi_{\text{opp}}^{\pm}$ angle. The resulting $\tilde{\gamma}_{\text{opp}}(\phi_i)$ curve is shown in Fig. 2. As can be observed, it approaches γ_{opp} much closer than the approximation (13) from [1].

Although the spread of γ_{opp} as function of α_i is the smallest for γ_{opp}, the drawback of using γ_{opp} to estimate ϕ_i is the limited range of ϕ_i, i.e. $\phi_i \leq \phi_{\text{opp}}$, for which we can obtain an estimate for ϕ_i. The ratio $\gamma_{\text{mid}} \triangleq \gamma_{j_{\text{mid}}}$ of the centre RE also has a small spread as function of α_i, and is non-zero for a larger range of ϕ_i than γ_{opp}. Therefore, the second coarse estimator for ϕ_i uses the ratio γ_{mid} to estimate ϕ_i in the interval $[0, \phi_{\text{mid}}]$, where $\phi_{\text{mid}} \approx \text{atan}\frac{2R_D}{h_A}$ is the incident angle above which the centre PD will no longer see the LED. Although the approximation (15) could be used, a better result is obtained when we approximate $A_0^{(j,i)}$ by

$$A_0^{(j,i)} \approx \pi R_D^2 - 2R_D d_{j,i} + \left(1 - \frac{\pi}{4}\right) d_{j,i}^2 \tag{18}$$

for $0 \leq d_{j,i} \leq 2R_D$. Similarly as for the previous estimator, we approximate $d_{j_{\max},i} \approx |d_{PD} - h_A \tan\phi_i|$, while $d_{j_{\text{mid}},i} \approx h_A \tan\phi_i$. This results in the function $\tilde{\gamma}_{\text{mid},1}(\phi_1)$ illustrated in Fig. 2. Inverting the function $\tilde{\gamma}_{\text{mid},1}(\phi_1)$ results in the estimator $\hat{\phi}_{i,\text{mid},1}(\gamma_{\text{mid}})$ given in (17), where $a = (\gamma_{\text{mid}} - 1)(1 - \pi/4)$, $b = -(\gamma_{\text{mid}} + 1) + \zeta\gamma_{\text{mid}}(1 - \pi/4)$, $b' = (\gamma_{\text{mid}} - 1) + \zeta\gamma_{\text{mid}}(1 - \pi/4)$, and $\gamma_{\text{mid}}^{\pm} = (1 - 2\zeta/\pi) + (1 - \pi/4)\zeta^2/\pi$. Depending on the system parameters, this approximation substantially deviates from the true γ_{mid} for small and/or large values of ϕ_i. Therefore, we apply a correction term, resulting in the estimator $\hat{\phi}_{i,\text{mid},2}(\gamma_{\text{mid}})$:

$$\hat{\phi}_{i,\text{mid},2}(\gamma_{\text{mid}}) = \begin{cases} \hat{\phi}_{i,\text{mid},1}(\gamma_{\text{mid}}) - \phi_{\text{corr}} \frac{\gamma_{\text{mid}}}{\gamma_{\text{corr}}} \\ \qquad\qquad \text{if } \gamma_{\text{mid}} \geq \gamma_{\text{mid}}^{\pm} \\ \hat{\phi}_{i,\text{mid},1}(\gamma_{\text{mid}}) - \phi_{\text{corr}} \left(\frac{\gamma_{\text{mid}}}{\gamma_{\text{corr}}} + \frac{\tau^6 - \tau}{\zeta^3}\right) \\ \qquad\qquad \text{if } \gamma_{\text{mid}} < \gamma_{\text{mid}}^{\pm} \end{cases}, \tag{19}$$

where $\gamma_{\text{corr}} = \tilde{\gamma}_{\text{mid}}(\phi_i = 0)$, $\phi_{\text{corr}} = \hat{\phi}_{i,\text{mid},1}(\gamma_{\text{corr}})$ and $\tau = \gamma_{\text{mid}}/\gamma_{\text{mid}}^{\pm}$, where $\gamma_{\text{mid}}^{\pm} = 1 - 2\zeta/\pi + (1 - \pi/4)\zeta^2/\pi$ is the value of γ_{mid} at the inflection point $\phi_{\text{mid}}^{\pm}$. Note that $\phi_{\text{mid}}^{\pm} = \phi_{\text{opp}}^{\pm}$, as this inflection point originates from the change in sign of $d_{PD} - h_A \tan\phi_i$ in $d_{j_{\max},i}$, present in the denominator of both γ_{opp} and γ_{mid}. The resulting approximation $\tilde{\gamma}_{\text{mid},2}(\phi_i)$ is also shown in Fig. 2, and resembles much closer γ_{mid}.

Although the second estimator for ϕ_i increases the range of ϕ_i over which an estimate can be obtained from ϕ_{opp} to ϕ_{mid}, the range is still substantially smaller than the maximum obtainable range ϕ_{out}. The only curves for γ_j that approach this maximum range are the curves $\gamma_{\max\pm1} \triangleq \gamma_{j_{\max}\pm1}$, which are non-zero for incident angles up to $\phi_{\max\pm1} \approx \text{atan}\frac{2R_D + d_{PD}\sqrt{2}/2}{h_A}$. However, the spread of $\gamma_{\max\pm1}$ as function of α_i is quite large, so inaccurate estimates of ϕ_i will be obtained when using these curves. Therefore, we propose as the third estimator $\hat{\phi}_{i,\text{ens}}$ for ϕ_i a combined approach. First, we note that in the derivations for the estimators, we did not take into account the shot noise. Hence, this implies that the estimates for ϕ_i are not reliable when γ_j is small. Taking this into account, we use the estimator (16) for incident angles in the interval $[0, \mu_{\text{opp}}\phi_{\text{opp}}]$, as the spread of γ_{opp} as function of α_i is smallest, where we select $\mu_{\text{opp}} = 0.95$ to avoid that the estimate is unreliable when γ_{opp} is noise dominated. Then, for the interval $\phi_i \in [\mu_{\text{opp}}\phi_{\text{opp}}, \mu_{\text{mid}}\phi_{\text{mid}}]$, with $\mu_{\text{mid}} = 0.98$, we apply estimator (19). Finally, for larger incident angles, we use the ratio $\gamma_{j_{\max}\pm1}$. To this end, we approximate $A_0^{(j,i)}$ by

$$A_0^{(j,i)} \approx \pi R_D^2 - \frac{2}{\pi} d_{j,i}^2 \tag{20}$$

for $0 \leq d_{j,i} \leq 2R_D$. Further, we approximate $d_{j_{\max}\pm1,i} \approx ((h_A \tan\phi_i)^2 + d_{PD}^2 - 2h_A \tan\phi_i\, d_{PD}\sqrt{2}/2)^{1/2}$, while $d_{j_{\max},i} \approx |d_{PD} - h_A \tan\phi_i|$, corresponding to $\tilde{\gamma}_{\max\pm1}(\phi_i)$, shown in Fig. 2. This results in the estimator

$$\hat{\phi}_{i,\max\pm1} = \text{atan}\left[\frac{R_D}{2h_A}\left(\zeta\rho - \sqrt{(\zeta\rho)^2 + 2(\pi^2 - 2\zeta^2)}\right)\right], \tag{21}$$

where $\rho = (2\gamma_{\max\pm1} - \sqrt{2})/(\gamma_{\max\pm1} - 1)$ and which will be used in the interval $\phi_i \in [\mu_{\text{mid}}\phi_{\text{mid}}, \mu_{\max\pm1}\phi_{\max\pm1}]$, with $\mu_{\max\pm1} = 1$.

IV. Numerical Results

In this section, we evaluate the performance of the three proposed coarse estimators. In our simulations, we assume $R_D = h_A = 1$ mm, $d_{PD} = 0.5R_D$, the optical power of the LEDs $A_i = 1$ W, a time interval $T = 10$ ms, $z_{S,i} - z_U = h = 2$ m, $R_p = 0.4$ mA/mW [21], a background spectral irradiance $p_n = 5.8 \times 10^{-6}$ W/cm^2·nm [20] and $\Delta\lambda = 360$ nm, for an optical filter placed in front of the PD that passes only visible light frequencies in the range 380 to 740 nm. This results in $N_0 = 8.4 \times 10^{-24}$ A^2/Hz.

First, we investigate the root of the mean squared error (rMSE) on the incident angle for a single LED positioned in the middle of a 6 m×6 m area, at a height $h = 2$ m above the receiver. The rMSE for the three coarse estimators and the coarse estimator from [1] is shown in Fig. 3. As can be observed, the estimator from [1] yields inaccurate estimates of the incident angle for small ($< \phi_{\text{opp}}^{\pm}$) and large ($\gtrapprox \phi_{\text{opp}}$) values of ϕ_i, but results in accurate estimates for intermediate values $\phi_{\text{opp}}^{\pm} < \phi_i \leq \phi_{\text{opp}}$. This is explained as the approximation $\tilde{\gamma}_{\text{opp}}(\phi_i)$ from [1] is close to the true γ_{opp} in the interval $[\phi_{\text{opp}}^{\pm}, \phi_{\text{opp}}]$, while the deviation is larger at small values of ϕ_i. The improved $\hat{\phi}_{i,\text{opp}}$ proposed in this

$$\hat{\phi}_{i,\text{opp}}(\gamma_{\text{opp}}) = \begin{cases} \text{atan}\left[\frac{1}{h_A}\left(R_D(3-\zeta)\lambda - \sqrt{(R_D(3-\zeta)\lambda)^2 - R_D^2(2-\zeta)(4-\zeta)}\right)\right] & \text{if } \gamma_{\text{opp}} \geq \gamma_{\text{opp}}^{\pm} \\ \text{atan}\left[\frac{1}{h_A}\left(R_D(3-\zeta\lambda) - \sqrt{(R_D(3-\zeta\lambda)^2 - R_D^2(8+\zeta^2-6\zeta\lambda)}\right)\right] & \text{if } \gamma_{\text{opp}} < \gamma_{\text{opp}}^{\pm} \end{cases} \tag{16}$$

$$\hat{\phi}_{i,\text{mid},1}(\gamma_{\text{mid}}) = \begin{cases} \text{atan}\left[\frac{R_D}{h_A a}\left(b + \sqrt{b^2 - a\left(\pi(\gamma_{\text{mid}}-1) - 2\zeta\gamma_{\text{mid}} + \zeta^2\gamma_{\text{mid}}(1-\frac{\pi}{4})\right)}\right)\right] & \text{if } \gamma_{\text{mid}} \geq \gamma_{\text{mid}}^{\pm} \\ \text{atan}\left[\frac{R_D}{h_A a}\left(b' + \sqrt{b'^2 - a\left(\pi(\gamma_{\text{mid}}-1) + 2\zeta\gamma_{\text{mid}} + \zeta^2\gamma_{\text{mid}}(1-\frac{\pi}{4})\right)}\right)\right] & \text{if } \gamma_{\text{mid}} < \gamma_{\text{mid}}^{\pm} \end{cases} \tag{17}$$

paper, performs better, especially for small incident angles ϕ_i, as the approximation matches better. Similarly as the estimator from [1], it is however not able to deliver reliable estimates for ϕ_i above ϕ_{opp}, corresponding to a horizontal distance to the LED of $h\tan\phi_{\text{opp}} = 3$ m. The estimators $\hat{\phi}_{i,\text{mid},2}$ and $\hat{\phi}_{i,\text{ens}}$ increase the range within which the incident angle can be estimated to ϕ_{mid} and $\phi_{\text{max}\pm1}$, which in our example corresponds to a horizontal distance $h\tan\phi_{\text{mid}} = 4$ m and $h\tan\phi_{\max\pm1} = 4.7$ m from the LED. However, in practice, the range $h\tan\phi_{\max\pm1} = 4.7$ m will not be reached, due to the lack of accuracy of the approximation $\tilde{\gamma}_{\max\pm1}(\phi_i)$. This can be observed in Fig. 3: $\hat{\phi}_{i,\text{ens}}(\phi_i)$ performs worse than $\hat{\phi}_{i,\text{mid},2}(\phi_i)$ for $\phi_i > \mu_{\text{mid}}\phi_{\text{mid}}$. In Fig. 3(c), the estimator $\hat{\phi}_{i,\text{mid},2}$ is used up to ϕ_{mid} and not to $\mu_{\text{mid}}\phi_{\text{mid}}$ as in Fig. 3(d). However, our simulations showed that when we increase the noise level, $\gamma_{\max\pm1}$ will be more reliable than γ_{mid} when $\phi_i > \mu_{\text{mid}}\phi_{\text{mid}}$, as it will be less affected by the noise. Furthermore, our simulations showed that, in general, $\hat{\phi}_{i,\text{ens}}(\phi_i)$ is more robust to noise than $\hat{\phi}_{i,\text{mid},2}(\phi_i)$. Note that with the levels μ_{opp}, μ_{mid} and $\mu_{\max\pm1}$, we can change the susceptibility of the estimator $\tilde{\gamma}_{\text{ens}}(\phi_i)$ to the noise. If the noise level strongly increases, μ_{opp}, μ_{mid} and $\mu_{\max\pm1}$ can be reduced to better cope with the noise excess.

Based on the coarse estimates for the AoA, we estimate the 3D position of the receiver using triangulation. We consider a 5 m $\times$ 5 m area, where four LEDs are placed in a square grid around the centre of the area and spacing between the LEDs 2.5 m. The receiver is placed $h = 2$ m below the LEDs. We estimate the polar angle with the algorithm from [1], and the incident angle with the different proposed algorithms. If an incident angle is larger than the largest incident angle that can be estimated with the coarse estimator, we neglect the LED in the triangulation phase, similarly as in [1]. If no reliable estimate for ϕ_i is available, for $i = 1, \ldots, K$, we set in the triangulation algorithm the estimated height $\hat{h}$ equal to 1.5 m. In Fig. 4, we show the cumulative distribution function of the 3D positioning error for the different coarse estimators for ϕ_i. As can be observed, the estimator from [1] yields the worst accuracy: only in slightly more than 50% of the positions, the positioning error is smaller than 30 cm. The proposed estimator $\hat{\phi}_{i,\text{opp}}$ slightly improves the performance, but the best performance is obtained with $\hat{\phi}_{i,\text{mid},2}$: in almost 90% of the positions, the positioning accuracy is better than 30 cm. The combination of estimators, i.e. $\hat{\phi}_{i,\text{ens}}$, performs worse than $\hat{\phi}_{i,\text{mid},2}$, mainly due to the larger deviations when $\phi_i > \mu_{\text{mid}}\phi_{\text{mid}}$. The results illustrate that, even when the AoAs are estimated with coarse estimators, the resulting positioning performance is fairly good.

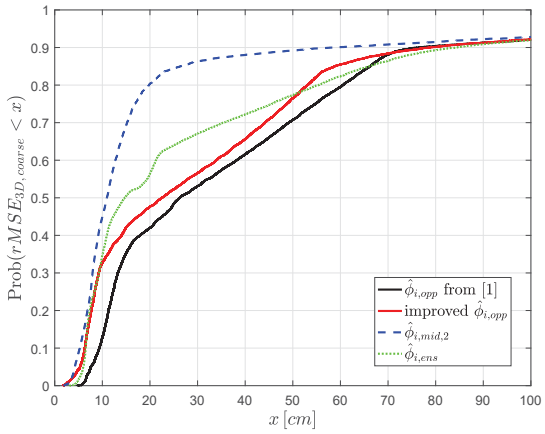

Fig. 4. Cumulative distribution function of the 3D positioning error based on $K = 4$ LEDs and coarse estimation of the AoA followed by triangulation, for $\epsilon = 5R_D$, $d_{PD} = 0.5R_D$ and $h_A = R_D = 1$ mm.

V. Conclusions

In this paper, we propose three coarse estimators for the incident angle for a VLP system with an aperture-based receiver with 9 REs. The derivation is based on simple approximations of the ratio γ_j, which is the ratio of the RSS value in RE j to the maximum of the RSS values in the outer REs. The resulting estimators have very low complexity, which allows real-time operation. The different coarse estimators proposed in this paper are evaluated with respect to the range within which they can accurately estimate the incident angle, and the accuracy of the estimate. Further, these coarse estimators are used to compute the position of the receiver through triangulation. The positioning accuracy that can be obtained is satisfactory: assuming 4 LEDs are used in a 5 m $\times$ 5 m area, a 3D positioning accuracy of 30 cm in almost 90% of the positions can be obtained for the best option.

References

[1] H. Steendam, "A 3D Positioning Algorithm for AOA-Based VLP with an Aperture-Based Receiver," *IEEE J. on Sel. Areas in Comm.*, special issue on Localisation, Communication and Networking with VLC, in press.

[2] J. Armstrong, Y. A. Sekercioglu and A. Neild, "Visible Light Positioning: A Roadmap for International Standardisation," *IEEE Communications Magazine*, Vol 51, No 12, pp. 68-73, Dec 2013.

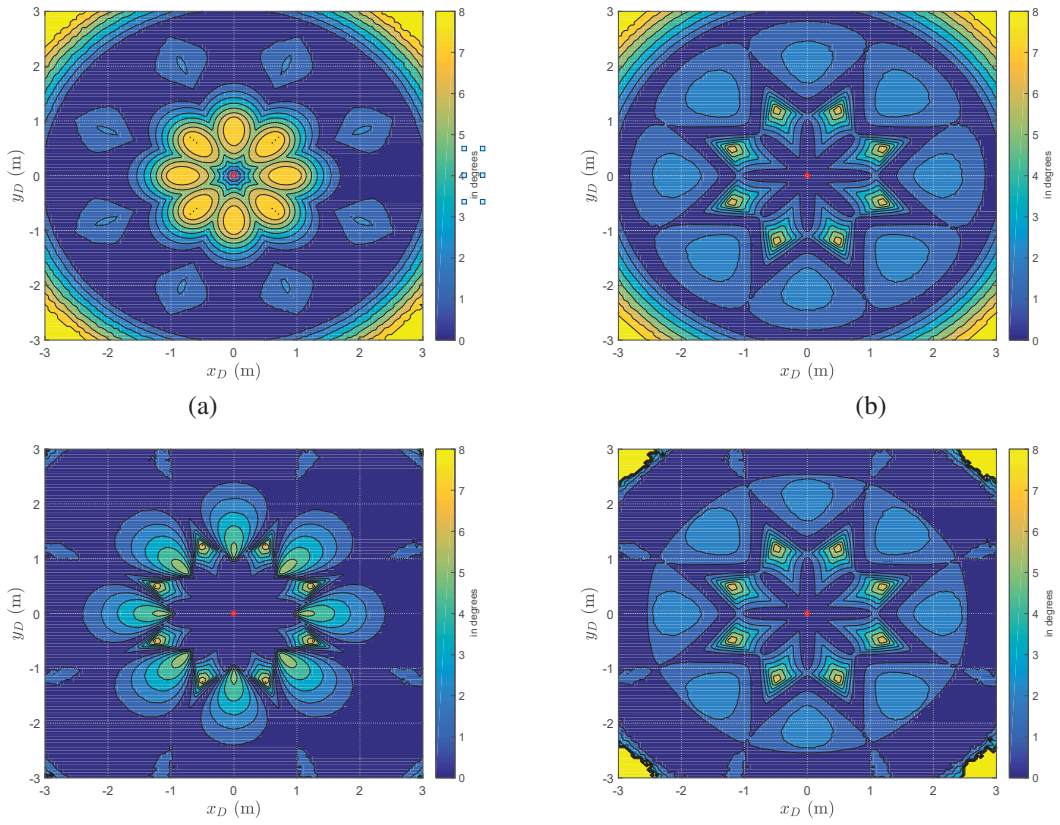

Fig. 3. rMSE on ϕ_i for a single LED in a 6 m×6 m area for $h = 2$ m, $d_{AP} = 5R_D$, $d_{PD} = 0.5R_D$ and $h_A = R_D = 1$ mm. The red dot is the position of the LED. (a) $\hat{\phi}_{i,\text{opp}}$ from [1], (b) improved $\hat{\phi}_{i,\text{opp}}$, (c) $\hat{\phi}_{i,\text{mid},2}$, (d) $\hat{\phi}_{i,\text{ens}}$ with $\mu_{\text{opp}} = 0.95$, $\mu_{\text{mid}} = 0.98$, $\mu_{\max \pm 1} = 1$.

[3] M. Biagi, S. Pergolini, A.-M. Vegni, "LAST: A Framework to Localize, Access, Schedule and Transmit in Indoor VLC Systems," *Journal of Lightwave Technology*, Vol 33, No 9, May 2015, pp. 1872-1887.

[4] S. Hann, J.-H. Kim, S.-Y. Jung, C.-S. Park, "White LED Ceiling Lights Positioning Systems for Optical Wireless Indoor Applications," in *Proc. ECOC 2010*, Torino, Italy, Sep 2010.

[5] S.-Y. Jung, S. Hann, C.-S. Park, "TDOA-Based Optical Wireless Indoor Localization Using LED Ceiling Lamps," *IEEE Transactions on Consumer Electronics*, Vol 57, No 4, pp. 1592-1597, Nov 2011.

[6] K. Panta, J. Armstrong, "Indoor Localization Using White LEDs," *Electronics Letters*, Vol 48, No 4, pp. 228-230, Feb 2012.

[7] A. Arafa, X. Jin, R. Klukas, "Wireless Indoor Optical Positioning With a Differential Photosensor," *IEEE Photonics Technology Letters*, Vol 32, No 14, pp. 2480-2485, Jul 2012.

[8] S.-Y. Jung, S. Hann, S. Park, C.-S. Park, "Optical Wireless Indoor Positioning System Using Light Emitting Diode Ceiling Lights," *Microwave and Optical Technology Letters*, Vol 54, No 7, pp. 1622-1626, Jul 2012.

[9] M. Rahaim, G.B. Prince, T.D.C. Little, "State Estimations and Motion Tracking for Spatially Diverse VLC Networks," in *Proc. Globecom Workshops*, Anaheim, CA, USA, Dec 2012, pp. 1249-1253.

[10] H.-S. Kim, D.-R. Kim, S.-H. Yang, Y.-H. Son, S.-K. Han, "An Indoor Visible Light Communication Positioning System Using a RF Allocation Technique," *Journal of Lightwave Technology*, Vol 31, No 1, pp. 134-144, Jan 2013.

[11] U. Nadeem, N.U. Hassan, M.A. Pasha, C. Yuen, "Highly Accurate 3D Wireless Indoor Positioning System Using White LED Lights," *Electronics Letters*, Vol 50, No 11, pp. 828-830, May 2014.

[12] G. Kail, P. Maechler, N. Preyss, A. Burg, "Robust Asynchronous Indoor Localization Using LED Lighting," in *Proc. IEEE International Conference on Acoustics, Speech and Signal Processing (ICASSP2014)*, Florence, Italy, May 2014.

[13] S.-H. Yang, H.-S. Kim, Y.-H. Son, and S.-K. Han, "Three-Dimensional Visible Light Indoor Localization Using AOA and RSS With Multiple Optical Receivers," *Journal of Lightwave Technology*, Vol 32, No 14, pp. 2480-2485, Jul 2014.

[14] M. Yasir, S.-W. Ho, B.N. Vellambi, "Indoor Positioning Using Visible Light and Accelerometer," *Journal of Lightwave Technology*, Vol 32, No 19, Oct 2014, pp. 3306-3316.

[15] Y.U. Lee, S.-M. Lee, "Random Distributed Angle-of-Arrival Parameter Estimation Technique for Visible Light Positioning," in *Proc. Int. Conf. on Telecom. and Sign. Proc., TSP2015*, Prague, Czech Rep., Jul 2015, pp. 467-471.

[16] M.F. Keskin, S. Gezici, "Comparative Theoretical Analysis of Distance Estimation in Visible Light Positioning Systems," *Journal of Lightwave Technology*, No. 3, Vol. 34, pp. 854-865, Feb 2016.

[17] D. Li, C. Gong, Z. Xu, "A RSSI-based indoor visible light positioning approach," in *Proc. 10th International Symposium on Communication Systems, Networks and Digital Signal Processing (CSNDSP)*, Prague, Czech Rep., Jul 2016.

[18] T.Q. Wang, C. He, J. Armstrong, "Angular Diversity for Indoor MIMO Optical Wireless Communications," in *Proc. IEEE International Conference on Communications (ICC2015)*, London, UK, Jun 2015.

[19] H. Steendam, T.Q. Wang, J. Armstrong, "Cramer-Rao Bound for AOA-Based VLP with an Aperture-Based Receiver," IEEE International Conference on Communications (ICC2017), Paris, France, May 2017.

[20] J.M. Kahn, J.R. Barry, "Wireless Infrared Communications," *Proceedings of the IEEE*, Vol 85, No 2, pp. 265-298, Feb 1997.

[21] L. Zeng, D.C. O'Brien, H.L. Minh, G.E. Faulkner, K. Lee, D. Jung, Y. Oh, E.T. Wong, "High Data Rate Multiple Input Multiple Output (MIMO) Optical Communications Using White LED Lighting," *IEEE Journal on Selected Areas in Communications*, Vol 27, No 9, pp. 1654-1662, Dec 2009.